

Copy No. 213  
RM No. L7K06

NACA RM No. L7K06  
c.1 (c. 2/13)

PLAIN FLAP



# RESEARCH MEMORANDUM

ENGINEERING LIBRARY  
CHANCE VOUGHT AIRCRAFT  
STRATFORD, CONN.

TWO-DIMENSIONAL WIND-TUNNEL INVESTIGATION AT HIGH  
REYNOLDS NUMBERS OF AN NACA 65A006  
AIRFOIL WITH HIGH-LIFT DEVICES

By

Robert J. Nuber and Stanley M. Gottlieb

Langley Memorial Aeronautical Laboratory  
Langley Field, Va.

CLASSIFIED DOCUMENT

This document contains classified information affecting the National Defense of the United States within the meaning of the Espionage Act, USC 50:31 and 32, the transmission or the revelation of its contents in any manner to an unauthorized person is prohibited by law. Information so classified may be imparted only to persons in the military and naval services of the United States, appropriate civilian officials and employees of the Federal Government who have a legitimate interest therein, and to United States citizens of known loyalty in the discretion of those who of necessity must be informed thereof.

## NATIONAL ADVISORY COMMITTEE FOR AERONAUTICS

WASHINGTON  
February 4, 1948

RM L7K06

2/9/48

NATIONAL ADVISORY COMMITTEE FOR AERONAUTICS

RESEARCH MEMORANDUM

TWO-DIMENSIONAL WIND-TUNNEL INVESTIGATION AT HIGH  
REYNOLDS NUMBERS OF AN NACA 65A006  
AIRFOIL WITH HIGH-LIFT DEVICES

By Robert J. Nuber and Stanley M. Gottlieb

SUMMARY

An investigation was made of an NACA 65A006 airfoil equipped with high-lift devices consisting of a 0.15-chord drooped-nose flap and a 0.20-chord plain trailing-edge flap. The airfoil section lift, pitching-moment, and drag characteristics obtained at high Reynolds numbers and low Mach numbers ( $M \leq 0.14$ ) with the flaps deflected individually and simultaneously are presented.

The results indicated that at Reynolds numbers up to  $9.0 \times 10^6$  the optimum combination of drooped-nose and plain trailing-edge flaps tested increased the maximum section lift coefficient from 0.78 to 1.89. The optimum combination of flap deflections obtained was  $28^\circ$  for the drooped-nose and  $59^\circ$  for the plain trailing-edge flap. The maximum section lift coefficient remained substantially constant between Reynolds numbers of  $3.0 \times 10^6$  and  $9.0 \times 10^6$  for the plain airfoil and the optimum combination of flap deflections tested but increased by approximately 0.08 as the Reynolds number was increased to  $18.0 \times 10^6$ .

Deflecting the drooped-nose flap was more effective than deflecting the plain trailing-edge flap in increasing the lift coefficient at which the drag increased rapidly. The section lift characteristics of both the NACA 65A006 and circular-arc airfoils are in good agreement. The main difference between these airfoils is that the drag of the NACA 65A006 airfoil is comparatively low up to much higher lift coefficients than is the case for the circular-arc airfoil.

INTRODUCTION

The use of thin airfoils on aircraft designed for the transonic and supersonic speed ranges has emphasized the need for the development

of means to increase the naturally low maximum lift of these profiles in order to obtain satisfactory low-speed characteristics.

The results of an investigation to determine the low-speed characteristics of two symmetrical circular-arc airfoils, 6 and 10 percent thick, equipped with leading-edge and trailing-edge flaps, are presented in reference 1. Recent data indicate that thin NACA 6-series airfoils have lower drag in the transonic speed range than circular-arc airfoils. The present investigation was therefore made to furnish the lift, drag, and pitching-moment characteristics of an NACA 65A006 airfoil with the 0.20-chord plain trailing-edge flap and the 0.15-chord drooped-nose flap deflected individually and in appropriate combinations for comparison with the circular-arc airfoil sections. These tests were made in the Langley two-dimensional low-turbulence tunnel, a variable-density wind tunnel which enables both the Reynolds number and Mach number appropriate to the landing condition for a typical airplane to be approximated simultaneously.

#### COEFFICIENTS AND SYMBOLS

$c_l$	section lift coefficient	$\left(\frac{l}{c_o c}\right)$
$c_d$	section drag coefficient	$\left(\frac{d}{q_o c}\right)$
$c_{m_c/4}$	section pitching-moment coefficient about the quarter chord	$\left(\frac{m_c/4}{q_o c^2}\right)$
$c_{m_{a.c.}}$	section pitching-moment coefficient about the aerodynamic center	$\left(\frac{m_{a.c.}}{q_o c^2}\right)$

where

$l$	lift per unit span
$d$	drag per unit span
$m$	pitching moment per unit span
$c$	chord of airfoil with flaps neutral
$q_o$	free-stream dynamic pressure $\left(\frac{\rho_o v_o^2}{2}\right)$
$\rho_o$	free-stream mass density

$V_0$	free-stream velocity
and	
$\alpha_0$	section angle of attack, degrees
$\delta$	flap deflection, degrees, positive when deflected below chord line
R	Reynolds number
$\Delta\alpha_{c_l \max}$	increment of section angle of attack at maximum lift due to flap deflection
$\Delta c_{l \max}$	increment of maximum section lift coefficient due to flap deflection

## Subscripts:

N	drooped-nose flap
F	plain trailing-edge flap

## MODEL

The model used in this investigation was a 24-inch chord NACA 65A006 airfoil equipped with a 15-percent chord drooped-nose flap and a 20-percent chord plain trailing-edge flap. Ordinates and photographs of the model are presented in table I and figures 1 and 2, respectively. Both flaps were pivoted on leaf hinges mounted flush with the lower surface. Model end plates, as shown in figure 1(a), were used to facilitate setting the deflection of the flaps. The model was designed so that plain trailing-edge flap deflections  $\delta_F$  up to  $59^\circ$  and drooped-nose flap deflections  $\delta_N$  up to  $47^\circ$  could be obtained. The flaps were sealed at the hinge line by having the flap skirt in rubbing contact with the flap.

The model surfaces were finished with number 400 carborundum paper; slight discontinuities, however, existed at the leaf hinges on the lower surface and at the line of contact between the flaps and flap skirts.

## TESTS

The tests were made in the Langley two-dimensional low-turbulence pressure tunnel. The tests included measurements of lift and pitching

moment at a Reynolds number of  $6.0 \times 10^6$  with the high-lift devices deflected either individually or in conjunction with one another. In addition, the lift characteristics were obtained at Reynolds numbers of 3.0, 9.0, 14.0, and  $18.0 \times 10^6$  with the flaps neutral and with the drooped-nose and plain trailing-edge flaps deflected simultaneously to  $28^\circ$  and  $59^\circ$ , respectively.

Drag measurements for the flaps neutral condition were obtained at Reynolds numbers of 3.0, 6.0, and  $9.0 \times 10^6$ . A further investigation of the drag characteristics was conducted at a Reynolds number of  $6.0 \times 10^6$  with the drooped-nose and plain trailing-edge flaps deflected as low-drag control flaps. For these tests, the high-lift devices were deflected both individually or in appropriate combinations through a range of deflections from  $0^\circ$  to  $20^\circ$ .

At Reynolds numbers of 3.0, 6.0, and  $9.0 \times 10^6$  the Mach number was substantially constant at 0.10. At Reynolds numbers of  $14.0 \times 10^6$  and  $18.0 \times 10^6$  the Mach numbers were 0.12 and 0.14, respectively. The airfoil lift, drag, and pitching-moment data were obtained and corrected to free air conditions by the methods described in reference 2.

## RESULTS AND DISCUSSION

Plain airfoil.— The section aerodynamic characteristics of the NACA 65A006 airfoil with the flaps neutral are presented in figures 3 and 4.

The maximum section lift coefficients remain approximately constant at 0.78 for Reynolds numbers of 3.0, 6.0, and  $9.0 \times 10^6$  whereas a favorable scale effect exists for Reynolds numbers above  $9.0 \times 10^6$  which increases the maximum section lift coefficient to a value of 0.85 at a Reynolds number of  $18.0 \times 10^6$ . At Reynolds numbers of 3.0, 6.0, and  $9.0 \times 10^6$ , it is believed that the small leading-edge radius of the NACA 65A006 airfoil causes separation much in the manner as occurs with a sharp leading edge. As the Reynolds number is increased, the round nose becomes effective and the same type of scale effect on the maximum section lift coefficient is observed on this airfoil as is observed on airfoils with larger leading-edge radius at lower Reynolds numbers. The jogs in the lift curve which originate at angles of attack of  $\pm 5^\circ$ , corresponding to a Reynolds number of  $6.0 \times 10^6$ , tend to move to higher angles of attack as the Reynolds number is increased. These jogs in the lift curves may be the result of the formation of a small local region of separated flow near the leading edge as discussed in reference 3.

The slope of the lift curves remains approximately constant at 0.106 as the Reynolds number is increased from  $3.0 \times 10^6$  to  $18.0 \times 10^6$ . At a Reynolds number of  $3.0 \times 10^6$  a slight discontinuity in the lift curve occurs near zero lift.

The quarter-chord pitching-moment data indicate that the aerodynamic center is located at the quarter-chord point of the airfoil. As is usually the case when an airfoil stalls, the center of pressure of the NACA 65A006 airfoil moves toward the rear and the quarter-chord moment coefficient increases negatively.

The minimum section drag coefficient remains approximately constant with increasing Reynolds number. At moderate lift coefficients, the variation in drag coefficient with Reynolds number is typical of that obtained on most NACA 6-series airfoils; however, at lift coefficients between 0.5 and 0.6 the drag rise is very rapid. The fact that the minimum drag of the NACA 65-006 airfoil, given in reference 4, is lower than that of the present model may be attributed to surface irregularities caused by the flap installation. These surface irregularities also cause the dissymmetry of the drag polars.

Airfoil with flaps deflected individually.- The lift and pitching-moment characteristics of the NACA 65A006 airfoil for various deflections of the drooped-nose and plain trailing-edge flaps deflected individually are presented in figures 5 and 6. The variation of the increment in maximum section lift coefficient  $\Delta c_{l_{max}}$  and increment of section angle of attack at maximum lift  $\Delta \alpha_{c_{l_{max}}}$  with deflection of the drooped-nose flap and the plain trailing-edge flap is summarized in figure 7.

As the 0.20-chord plain trailing-edge flap was deflected (fig. 5), the maximum section lift coefficients increased while the angles of attack for maximum lift decreased. The maximum section lift coefficient obtained was 1.62 which appears to be very nearly the optimum. For plain trailing-edge flap deflections up to  $20^\circ$ , the flow over the flap appears to be unseparated at low angles of attack and the increment in lift coefficient due to flap deflection is large. As angles of attack near maximum lift are reached, it is believed that the flow over the flap becomes separated as indicated by the decrease in flap effectiveness. Deflecting the plain trailing-edge flap from  $20^\circ$  to  $29^\circ$  and above caused the flow over the flap to become separated over the entire range of angles of attack as indicated by the decrease in flap effectiveness (fig. 5). Increasing the plain trailing-edge flap deflections above  $29^\circ$  produced increments in the section lift coefficient of the magnitude expected for separated flow. The jogs, shown on the curves for plain trailing-edge flap deflections of  $49^\circ$  and  $59^\circ$ , have been observed on

other airfoils with plain flaps. The sudden increases in the slope of the lift curves, particularly for flap deflections of  $29^\circ$  and above for angles of attack near maximum lift, are similar to those observed for 6-percent-thick airfoils with split flaps (reference 4).

Deflecting the drooped-nose flap (fig. 6) increased the maximum section lift coefficients and increased the angles of attack for maximum lift by alleviating the negative pressure peaks that cause leading-edge separation near maximum lift. These pressure peaks are alleviated because the flow approaching the leading edge is more nearly aligned at high angles of attack when the drooped-nose flap is deflected. With the drooped-nose flap deflected  $47^\circ$  the maximum section lift coefficient corresponding to a Reynolds number of  $6.0 \times 10^6$  is 1.19. Figure 7 shows that the maximum section lift coefficient is substantially the same for drooped-nose flap deflections above  $28^\circ$ . At angles of attack well below those for maximum lift (fig. 6), the drooped-nose flap acts as a spoiler on the lower surface of the airfoil which causes some reduction in lift. These losses in lift increase as the drooped-nose flap deflection is increased.

The pitching-moment characteristics presented in figures 5 and 6 with either the drooped-nose flap or the plain trailing-edge flap deflected indicate that the aerodynamic center tends to move toward the leading edge for angles of attack less than but approaching the angle of attack for maximum lift. The unusual variation of the pitching-moment curves with flap deflection for plain trailing edge flap deflections of  $20^\circ$  and  $29^\circ$  (fig. 5) is associated with the separation which caused a similar phenomenon in the lift characteristics.

Airfoil with flaps deflected in combination.- The results of the investigation in which the drooped-nose and plain trailing-edge flaps were deflected simultaneously in various combinations are presented in figure 8. It can be seen by reference to figure 8 that the optimum flap configuration tested, corresponding to the highest maximum section lift coefficient, was  $\delta_N = 28^\circ$ ,  $\delta_F = 59^\circ$ . In view of this result, a series of tests were made to determine the scale effect on maximum lift with the drooped-nose and plain trailing-edge flaps deflected  $28^\circ$  and  $59^\circ$ , respectively. These data, presented in figure 9, show that the maximum section lift coefficient for Reynolds numbers of 3.0, 6.0, and  $9.0 \times 10^6$  remains approximately constant at a value of 1.89. The maximum section lift coefficient, however, increases with increasing Reynolds number between Reynolds numbers of  $9.0 \times 10^6$  and  $18.0 \times 10^6$  by approximately 0.08. This phenomenon is similar to that for the flaps neutral condition.

With the plain trailing-edge flap deflected  $59^\circ$ , the increment in the maximum section lift coefficient and the angle of attack for maximum lift obtained by deflecting the drooped-nose flap from  $0^\circ$  (fig. 5) to  $28^\circ$  (fig. 8) is 0.27 and  $5^\circ$ , respectively. This increment

in maximum section lift coefficient is about 67 percent of that obtained by deflecting the drooped-nose flap from  $0^\circ$  to  $28^\circ$  (fig. 6) when the plain trailing-edge flap is in the neutral position.

The section pitching-moment characteristics of the airfoil at combined flap deflections of  $\delta_N = 28^\circ$ ,  $\delta_F = 59^\circ$  (fig. 8) show that the aerodynamic center remains ahead of the quarter-chord point in the angle-of-attack range from about  $-3^\circ$  to  $11^\circ$ . In addition, the combined action of the drooped-nose flap and plain trailing-edge flap caused stable pitching-moment characteristics at angles of attack less than  $-3^\circ$  and greater than  $11^\circ$ .

Effect of small flap deflections on drag.- The lift and drag characteristics of the NACA 65A006 airfoil with the drooped-nose and plain trailing-edge flaps deflected individually and in various combinations are presented in figure 10. Deflecting the drooped-nose flap  $5^\circ$ ,  $9^\circ$ , and  $19^\circ$  caused no appreciable change in the section drag coefficient of the airfoil at a lift coefficient of 0.30, but progressive increases in the lift coefficient at which the drag increased rapidly were obtained. This result is attributed to the drooped-nose flap delaying the formation of a negative pressure peak at the leading edge as it is deflected. In general, deflecting the drooped-nose flap was more effective than was deflecting the plain trailing-edge flap in increasing the lift coefficient at which the drag increased rapidly.

The lift and pitching-moment characteristics of the airfoil for two combined deflections of the drooped-nose and plain trailing-edge flaps which showed the greatest increase in the lift coefficient at which the drag increased rapidly are presented in figure 11.

Comparison with circular-arc airfoil.- Some of the results of the present investigation are compared in figure 12 with those obtained from tests of the 6-percent-thick circular-arc airfoil (reference 1), designated NACA 2S-(50)(03)-(50)(03). These data indicate that the section lift characteristics of both airfoils are in good agreement. The pitching-moment characteristics show that the aerodynamic center of the circular-arc airfoil is nearer the leading edge than that of the NACA 6-series airfoil. The major differences between the two airfoils occur in the drag characteristics (not compared herein) where the magnitude of the drag of the NACA 6-series airfoil is comparatively low up to much higher lift coefficients than is the case for the circular-arc airfoil.

It is believed that the air loads on the drooped-nose flap of the NACA 65A006 airfoil may be greater than those on the drooped-nose flap of the NACA 2S-(50)(03)-(50)(03) airfoil (reference 5) at the high Reynolds numbers only because the magnitude of the peak pressures near the leading edge of the NACA 6-series airfoil probably will not be limited by separation.



## CONCLUSIONS

The results of a two-dimensional wind-tunnel investigation at Reynolds numbers from  $3.0 \times 10^6$  to  $18.0 \times 10^6$  of an NACA 65A006 airfoil equipped with a leading-edge flap and a trailing-edge flap indicate the following conclusions:

1. At Reynolds numbers up to  $9.0 \times 10^6$ , the optimum combination of drooped-nose and plain trailing-edge flaps tested increased the maximum section lift coefficients from 0.78 to 1.89.

2. The optimum combination of flap deflections obtained was  $28^\circ$  for the drooped-nose flap and  $59^\circ$  for the plain trailing-edge flap.

3. The maximum section lift coefficient remained substantially constant between Reynolds numbers of  $3.0 \times 10^6$  and  $9.0 \times 10^6$  for the plain airfoil and the optimum combination of flap deflections tested but increased by approximately 0.08 as the Reynolds number was increased to  $18.0 \times 10^6$ .

4. Deflection of the drooped-nose flap was more effective than was deflection of the plain trailing-edge flap in increasing the lift coefficient at which the drag increased rapidly.

5. The section lift characteristics of both the NACA 65A006 and circular-arc airfoils are in good agreement. The main difference between these airfoils is that the drag of the NACA 65A006 airfoil is comparatively low up to much higher lift coefficients than is the case for the circular-arc airfoil.

Langley Memorial Aeronautical Laboratory  
National Advisory Committee for Aeronautics  
Langley Field, Va.

## REFERENCES

1. Underwood, William J., and Nuber, Robert J.: Two-Dimensional Wind-Tunnel Investigation at High Reynolds Numbers of Two Symmetrical Circular-Arc Airfoil Sections with High-Lift Devices. NACA RM No. L6K22, 1947.
2. von Doenhoff, Albert E., and Abbott, Frank T., Jr.: The Langley Two-Dimensional Low-Turbulence Pressure Tunnel. NACA TN No. 1283, 1947.
3. von Doenhoff, Albert E., and Tetervin, Neal: Investigation of the Variation of Lift Coefficient with Reynolds Number at a Moderate Angle of Attack on a Low-Drag Airfoil. NACA CB, Nov. 1942.
4. Abbott, Ira H., von Doenhoff, Albert E., and Stivers, Louis S., Jr.: Summary of Airfoil Data. NACA ACR No. L5C05, 1945.
5. Underwood, William J., and Nuber, Robert J.: Aerodynamic Load Measurements over Leading-Edge and Trailing-Edge Plain Flaps on a 6-Percent-Thick Symmetrical Circular-Arc Airfoil Section. NACA RM No. L7H04, 1947.

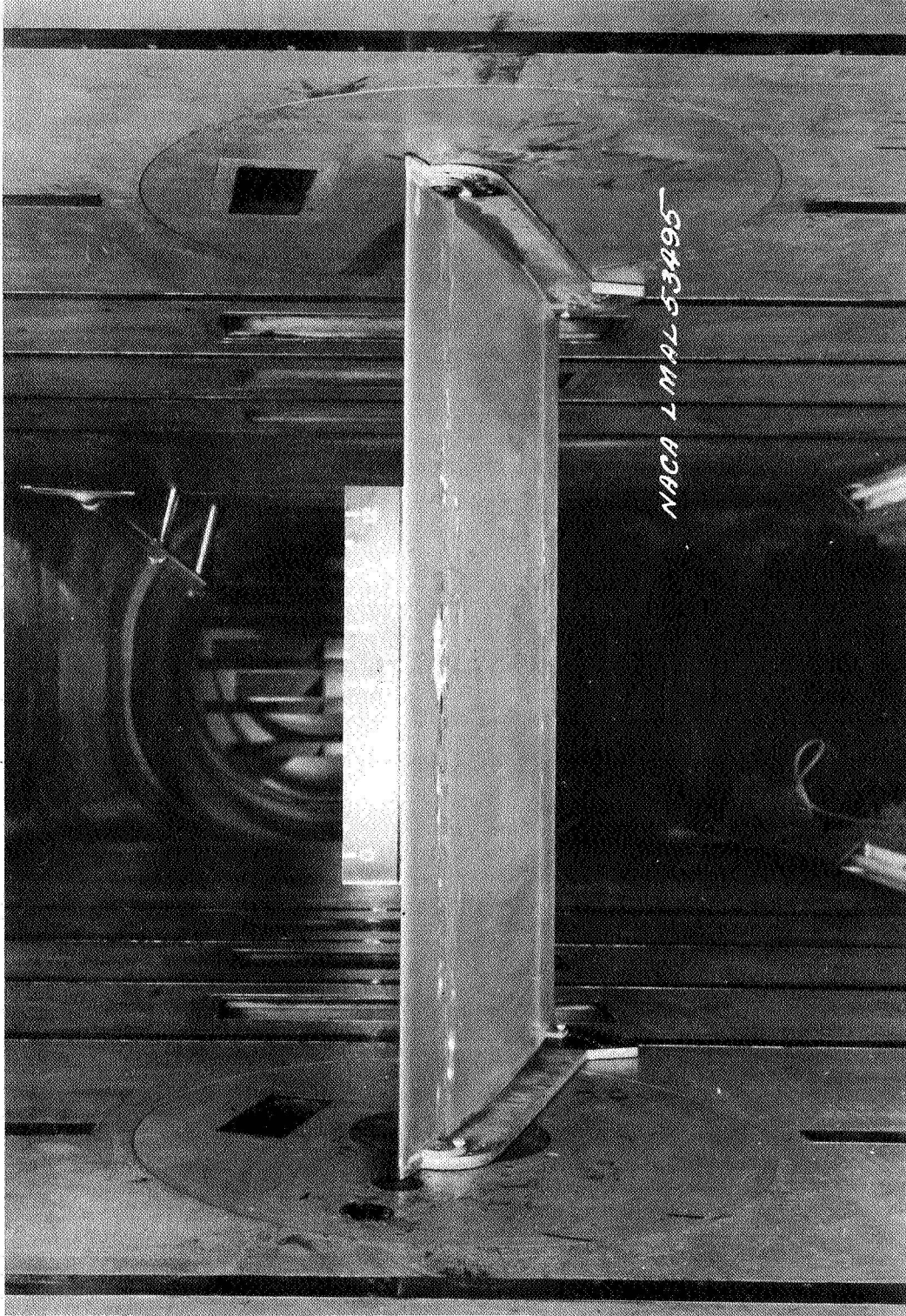
TABLE I

## ORDINATES FOR THE NACA 65A006 AIRFOIL

[Stations and ordinates given in percent of airfoil chord]

Station	Upper surface	Lower surface
0	0	0
.5	.464	-.464
.75	.563	-.563
1.25	.718	-.718
2.5	.981	-.981
5	1.313	-1.313
7.5	1.591	-1.591
10	1.824	-1.824
15	2.194	-2.194
20	2.474	-2.474
25	2.687	-2.687
30	2.842	-2.842
35	2.945	-2.945
40	2.996	-2.996
45	2.992	-2.992
50	2.925	-2.925
55	2.793	-2.793
60	2.602	-2.602
65	2.364	-2.364
70	2.087	-2.087
75	1.775	-1.775
80	1.437	-1.437
85	1.083	-1.083
90	.727	-.727
95	.370	-.370
100	0	0
L. E. Radius: 0.229		
T. E. Radius: 0.014		

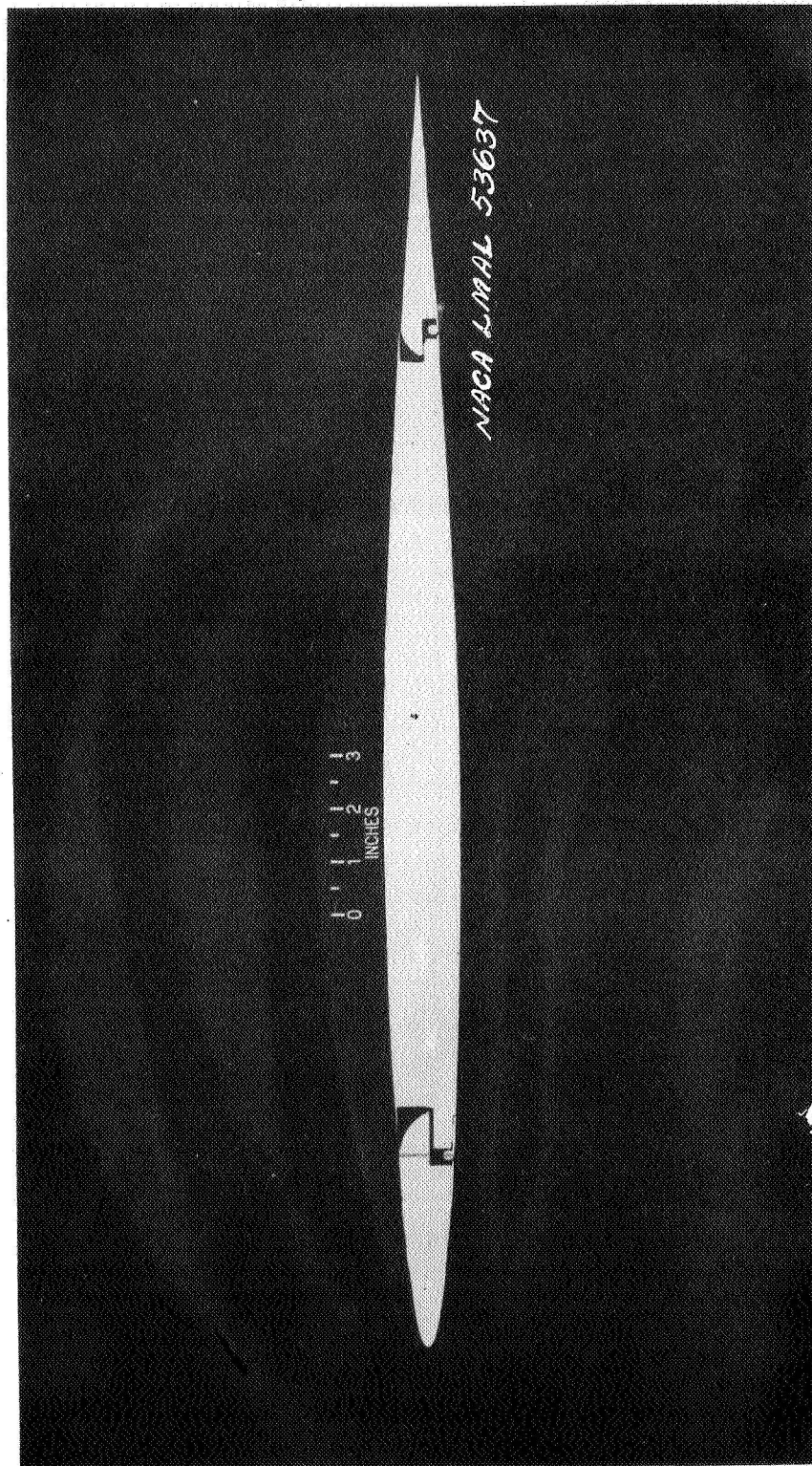




(a) Front bottom view.

Figure 1.- NACA 65A006 airfoil with 0.15-chord drooped-nose and 0.20-chord plain trailing-edge flaps neutral.

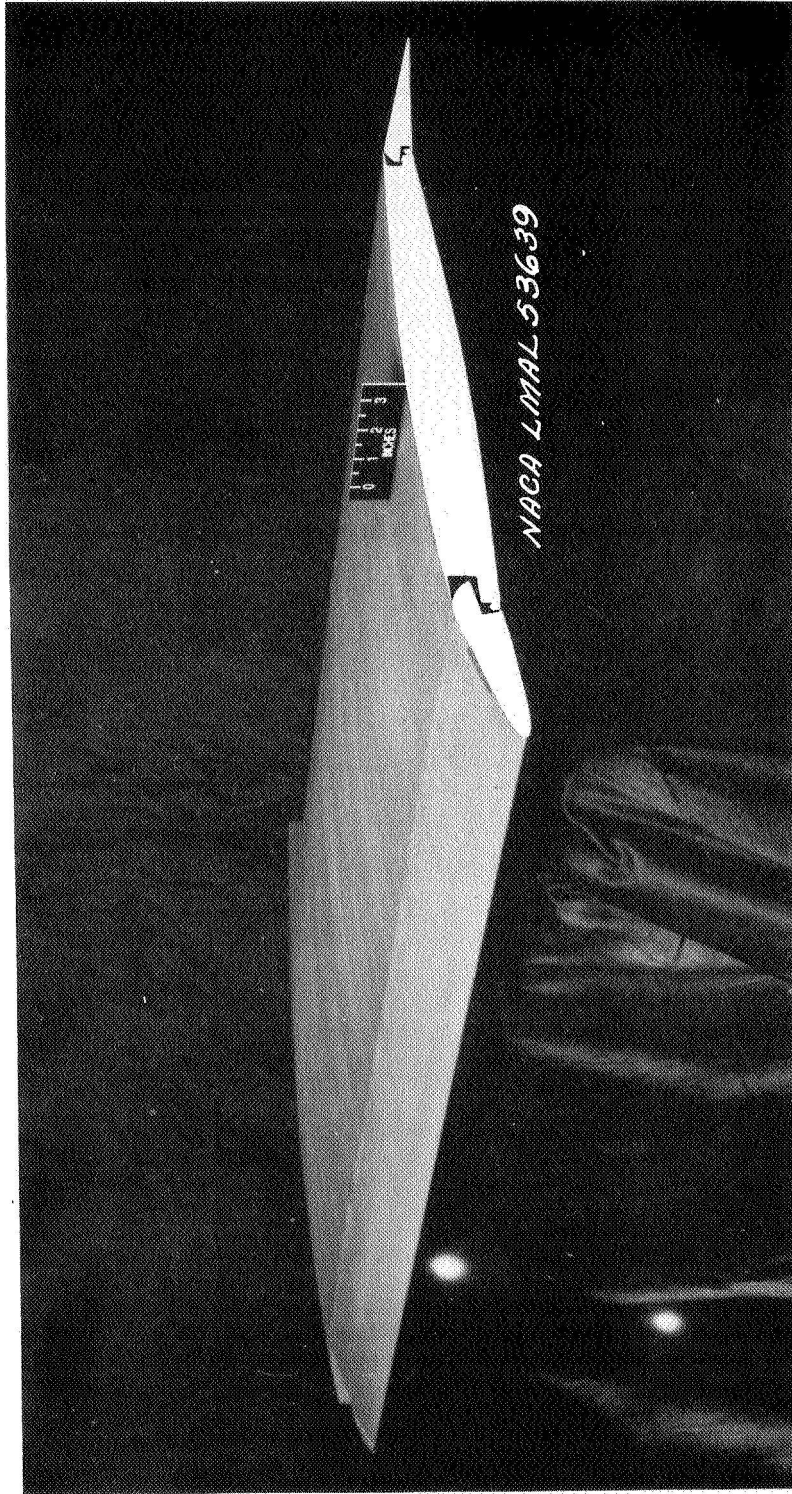




(b) Profile view.

Figure 1.- Concluded.



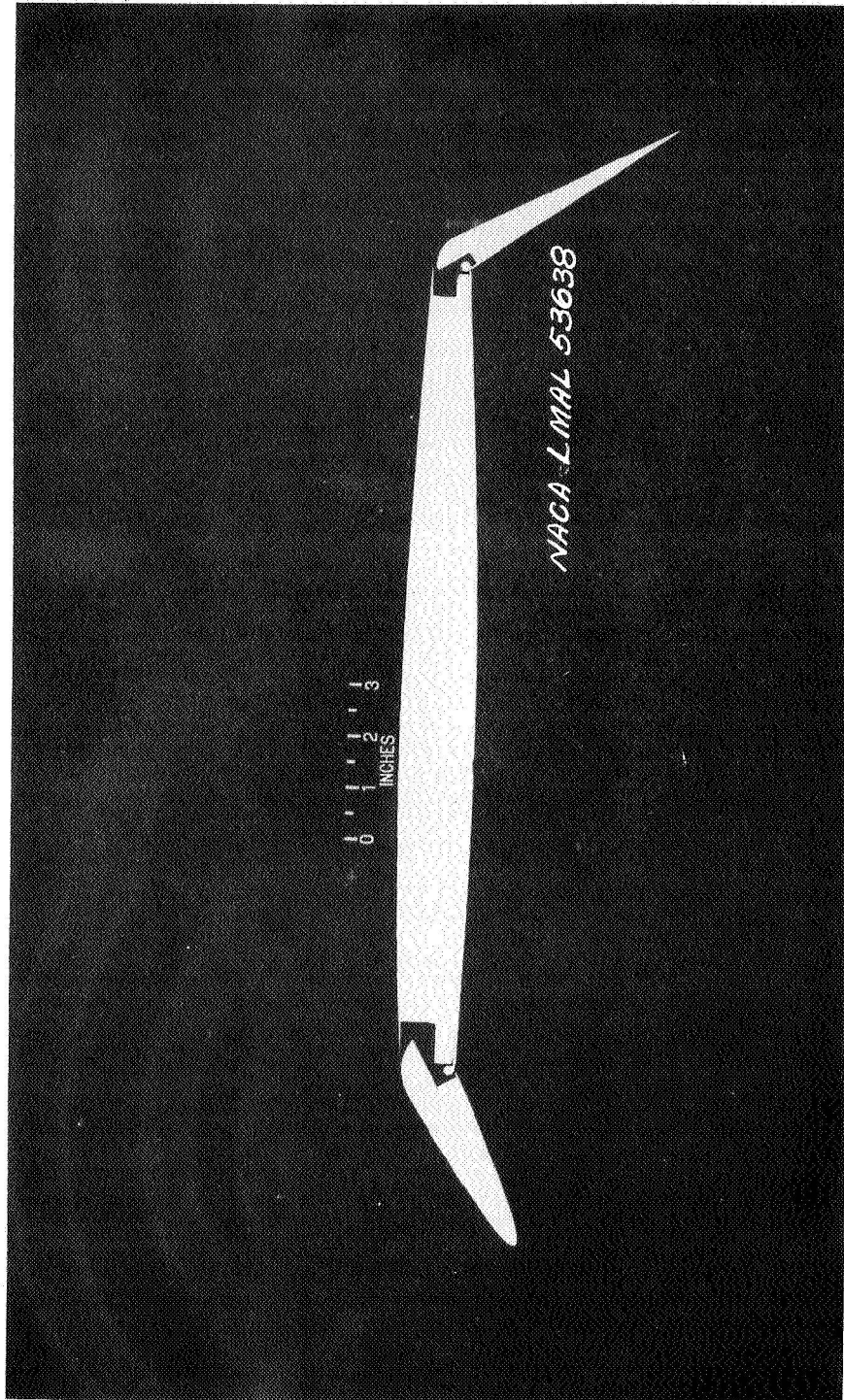


(a) Three-quarter front view of upper surface;  $\delta_N = \delta_F = 10^\circ$ .

Figure 2.- NACA 65A006 airfoil with 0.15-chord drooped-nose and 0.20-chord plain trailing-edge flaps deflected.







(b) Profile view.  $\delta_N = 28^\circ$ ;  $\delta_F = 59^\circ$ .

Figure 2.- Concluded.



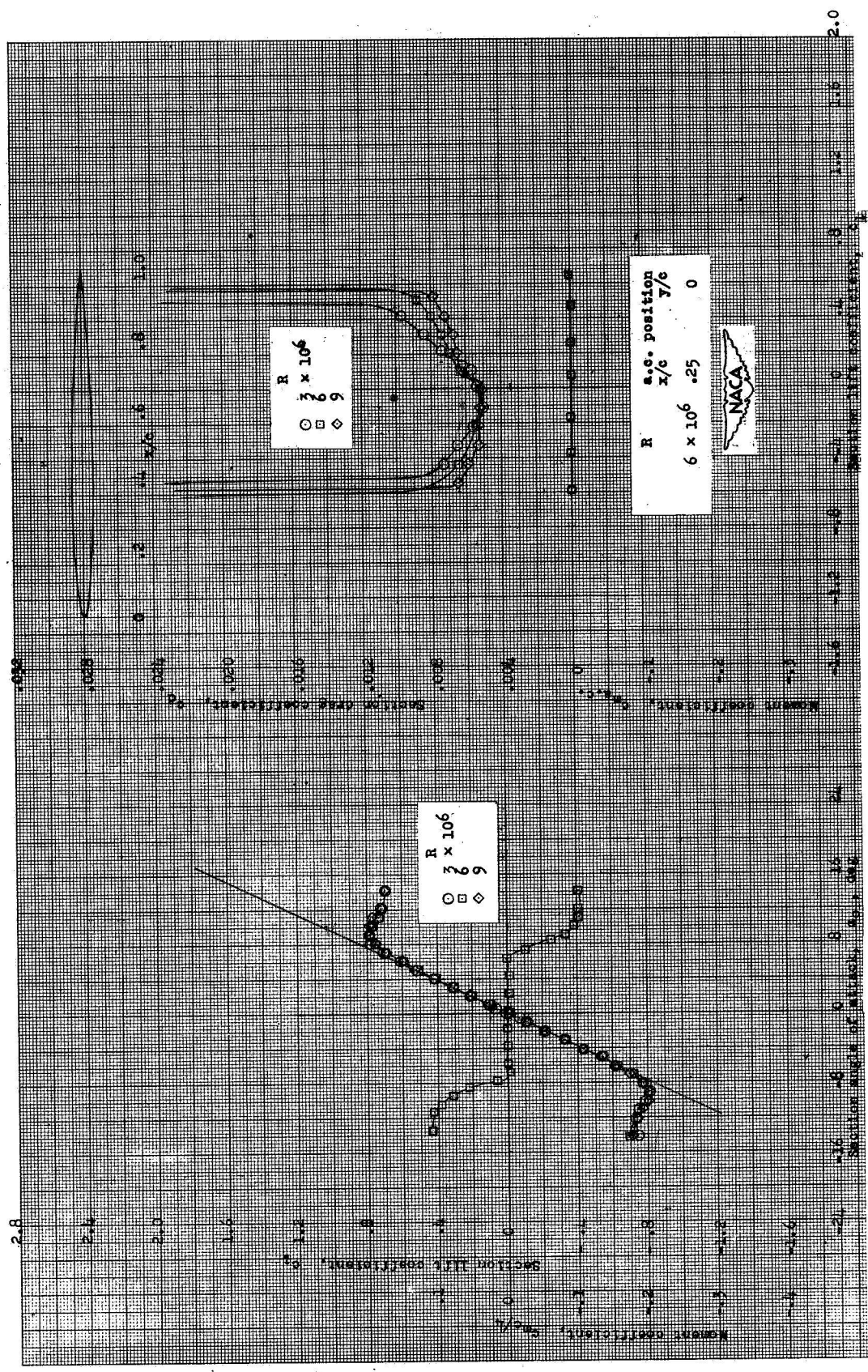
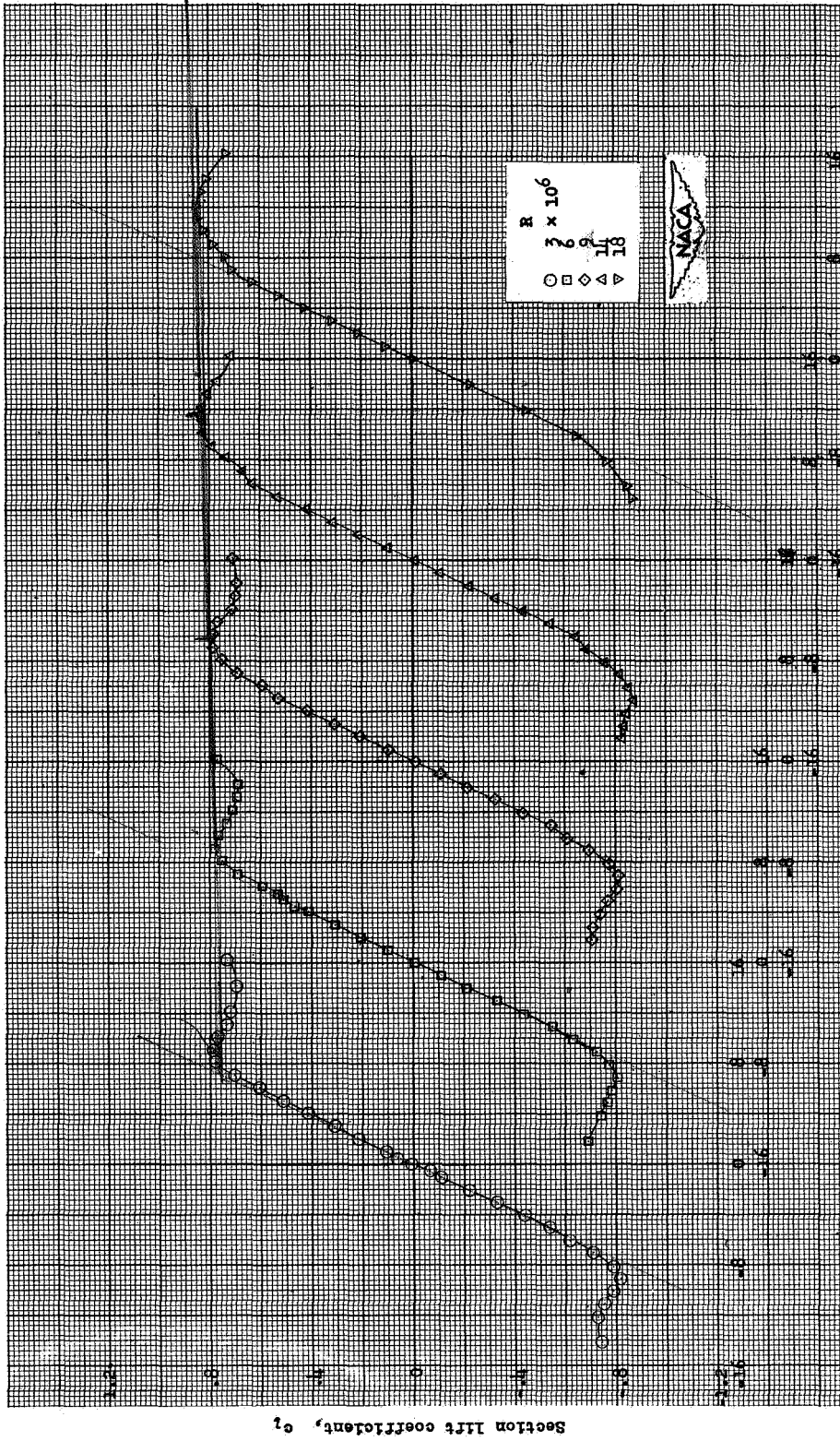


Figure 3.- Aerodynamic characteristics of an NACA 65A006 airfoil.

*Cr<sub>2</sub> = 104*



Section angle of attack,  $\alpha$ , deg  
Figure 4.- Effect of increased Reynolds number on the section lift characteristics of an NACA 65A006 airfoil with the drooped-nose and plain flaps neutral.

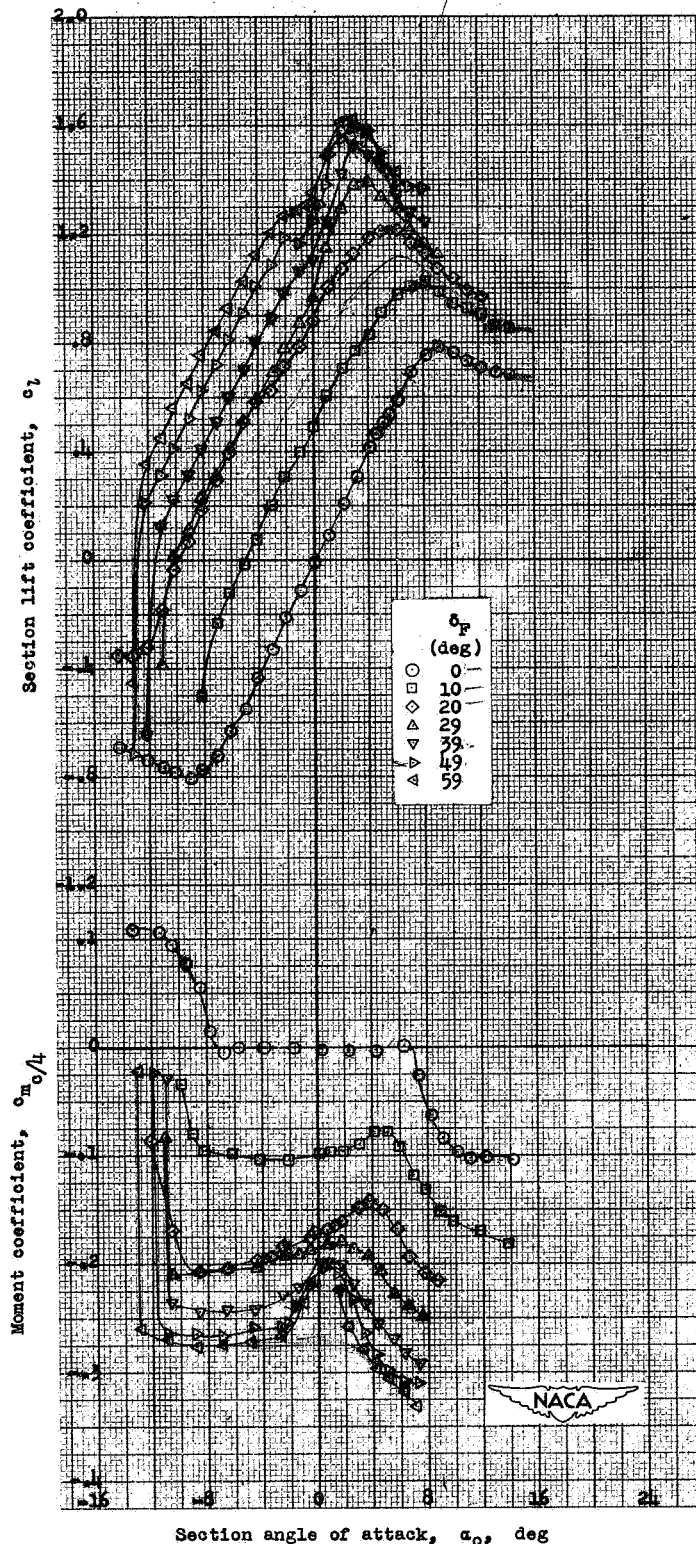


Figure 5.- Section lift and pitching-moment characteristics of an NACA 65A006 airfoil for various deflections of the 0.20-chord plain flap;  $\delta_N, 0^\circ$ ;  $R, 6 \times 10^6$ .

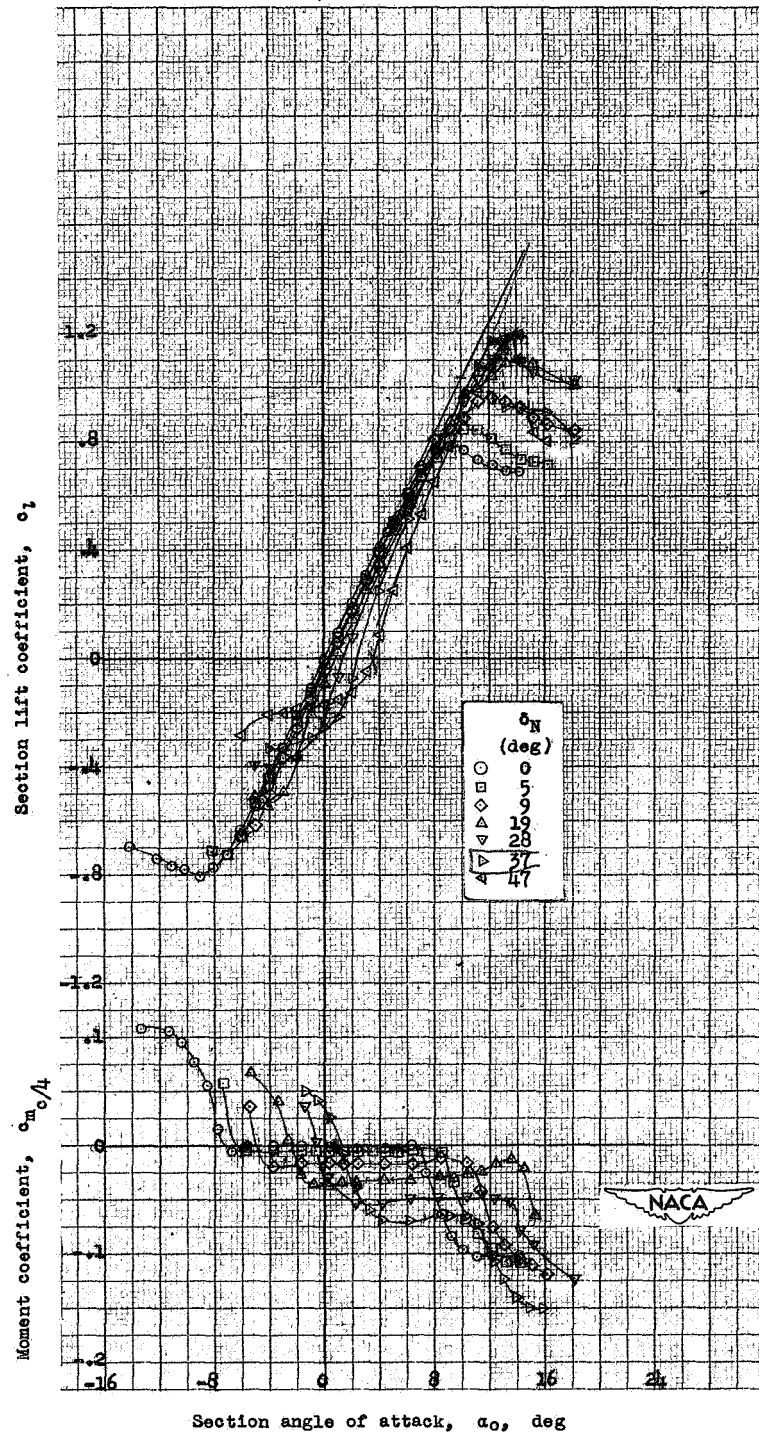


Figure 6.- Section lift and pitching-moment characteristics of an NACA 65A006 airfoil for various deflections of the 0.15-chord drooped-nose flap;  $\delta_F, 0^\circ$ ;  $R, 6 \times 10^6$ .

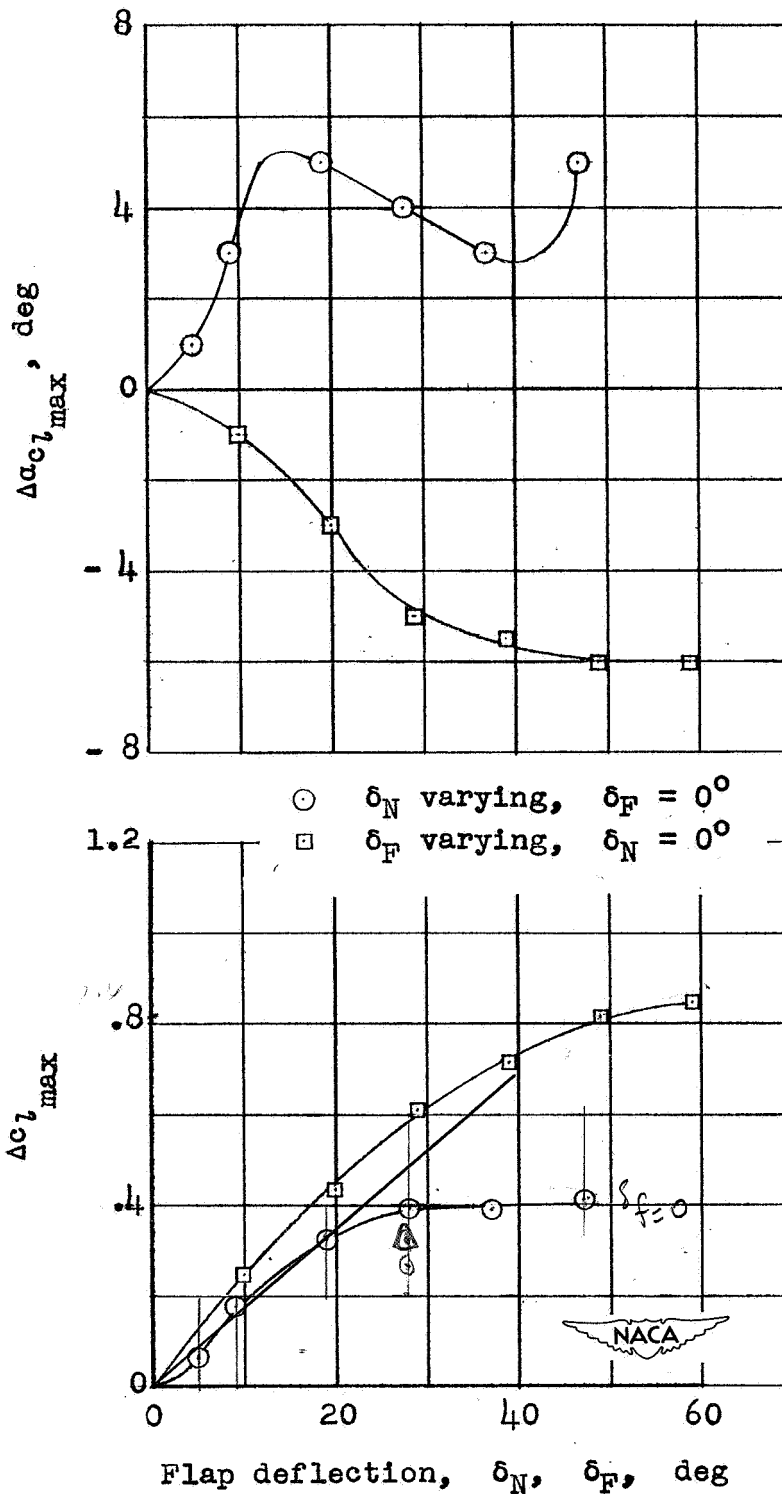


Figure 7.- Variation of the increment in maximum section lift coefficient and angle of stall with deflection of the drooped-nose and plain flaps on an NACA 65A006 airfoil;  $R. 6 \times 10^6$ .



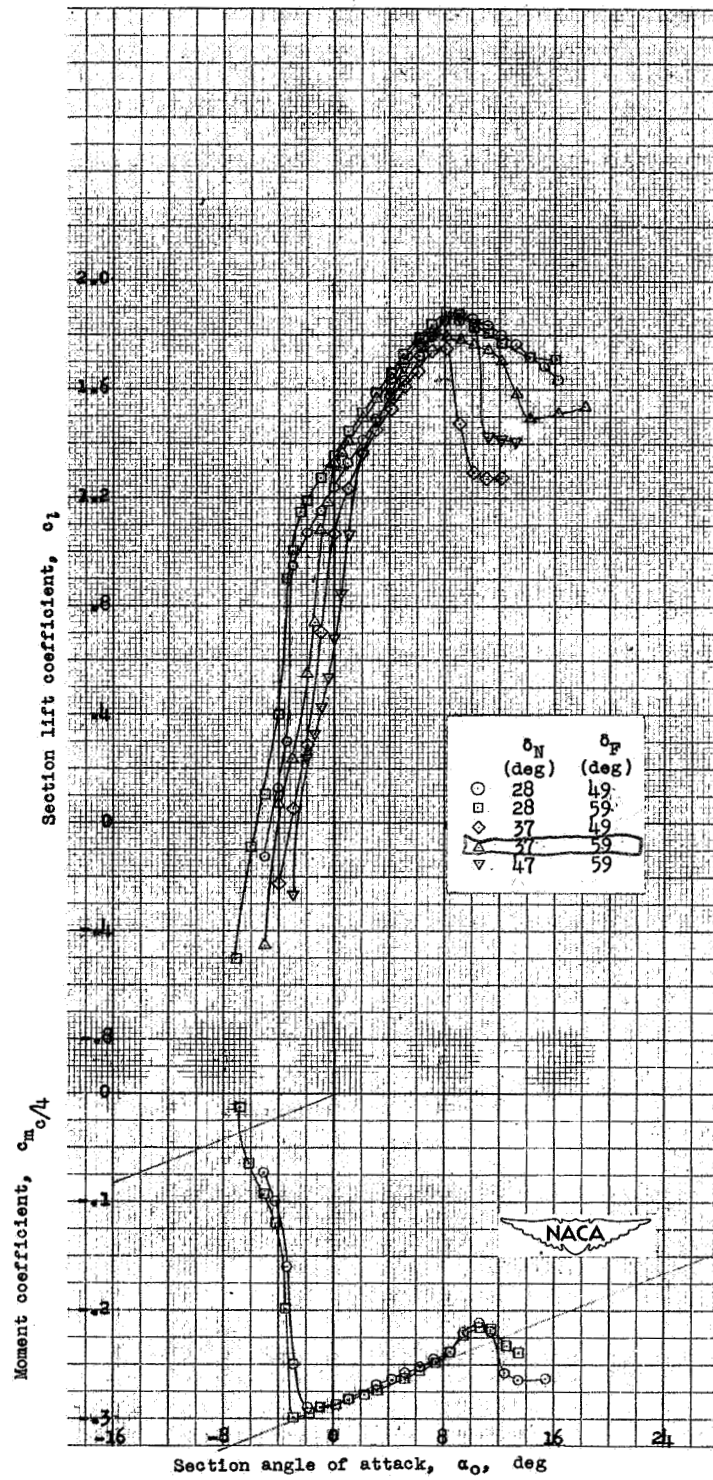


Figure 8.- Section lift and pitching-moment characteristics of an NACA 65A006 airfoil for various deflections of the drooped-nose and plain flaps;  $R, 6 \times 10^6$ .

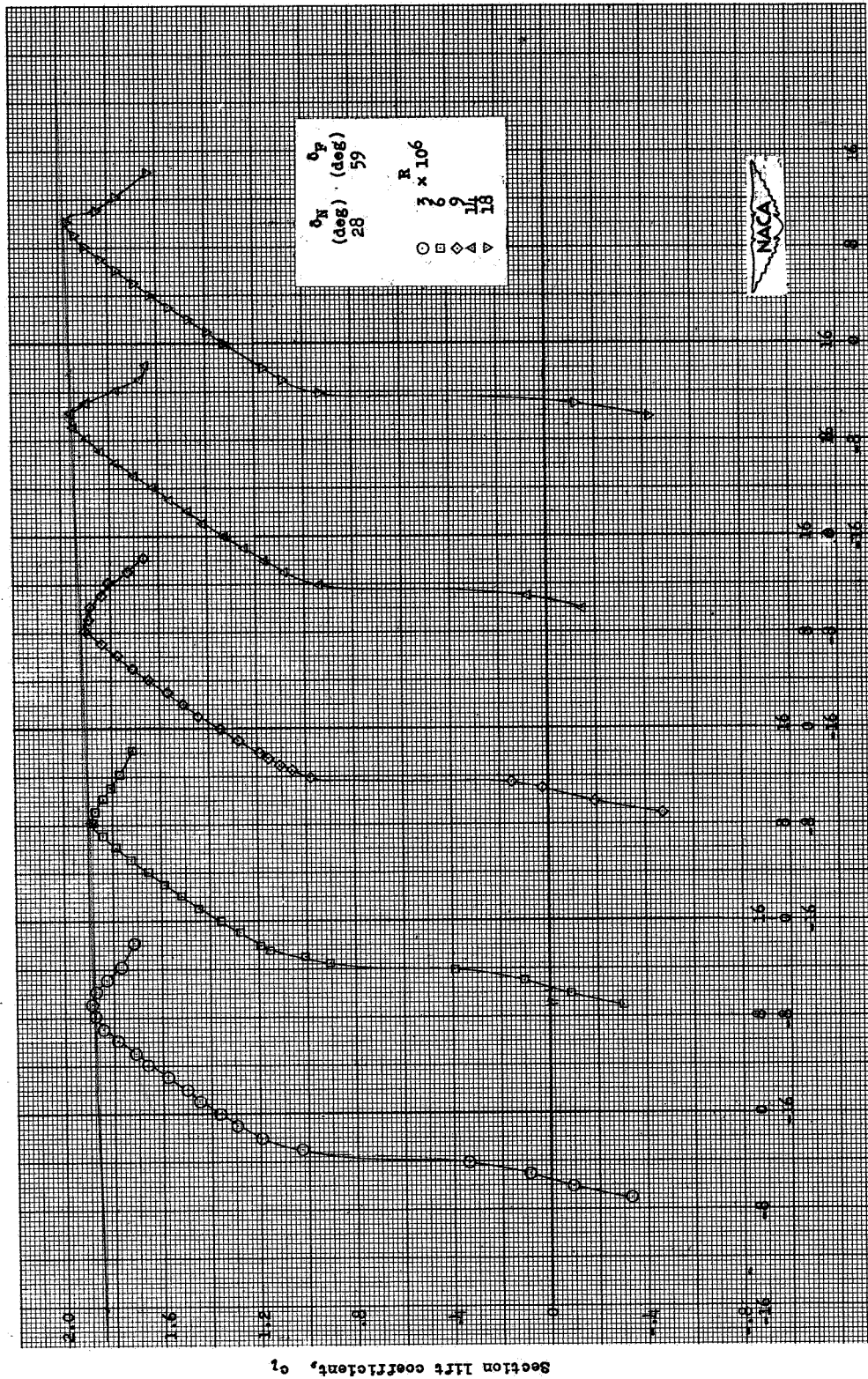


Figure 9 .- Effect of increased Reynolds number on the section lift characteristics of an NACA 65A006 airfoil with the drooped-nose and plain flaps deflected simultaneously.

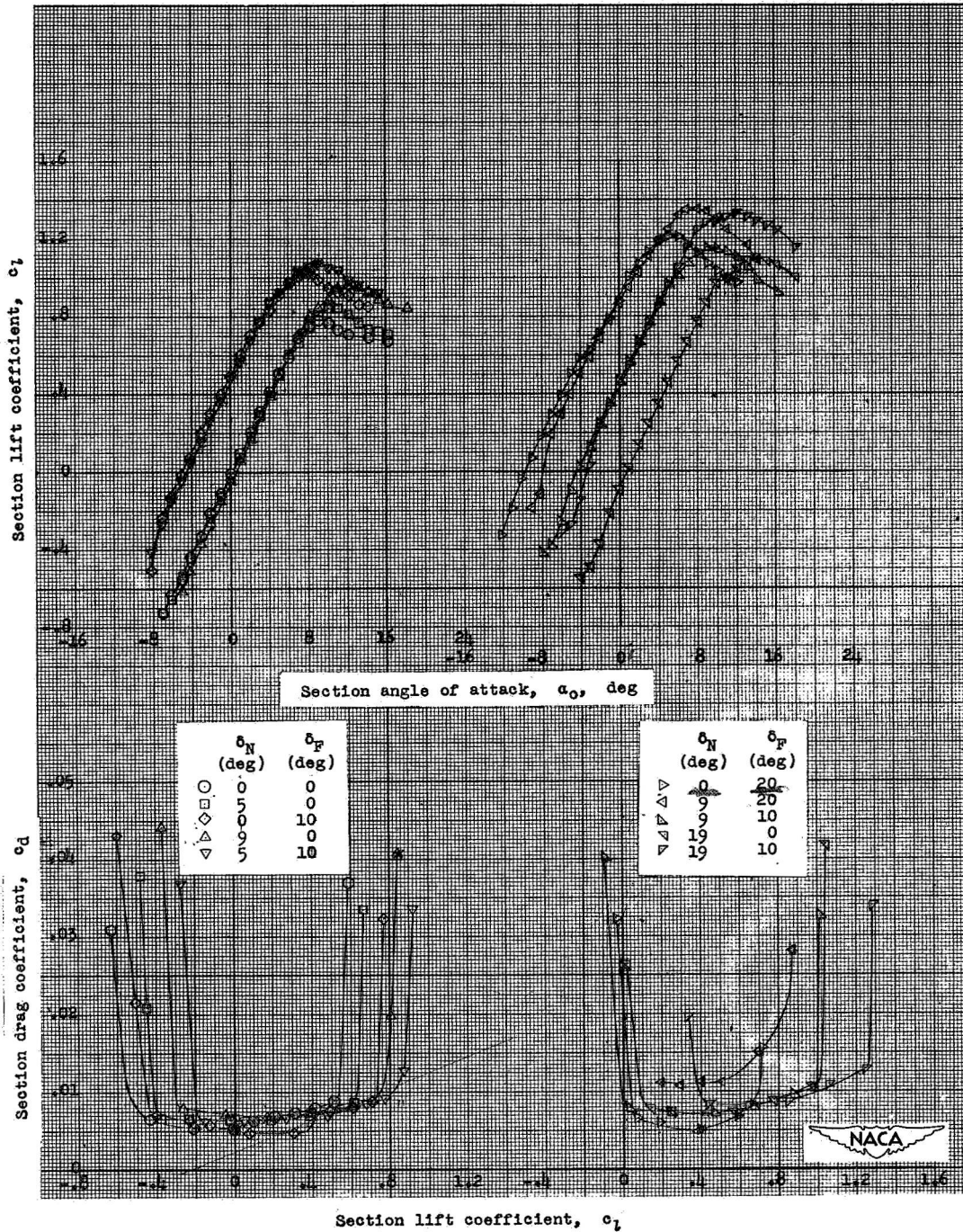


Figure 10.- Section lift and drag characteristics of an NACA 65A006 airfoil for various deflections of the drooped-nose and plain flaps;  $R, 6 \times 10^6$ .

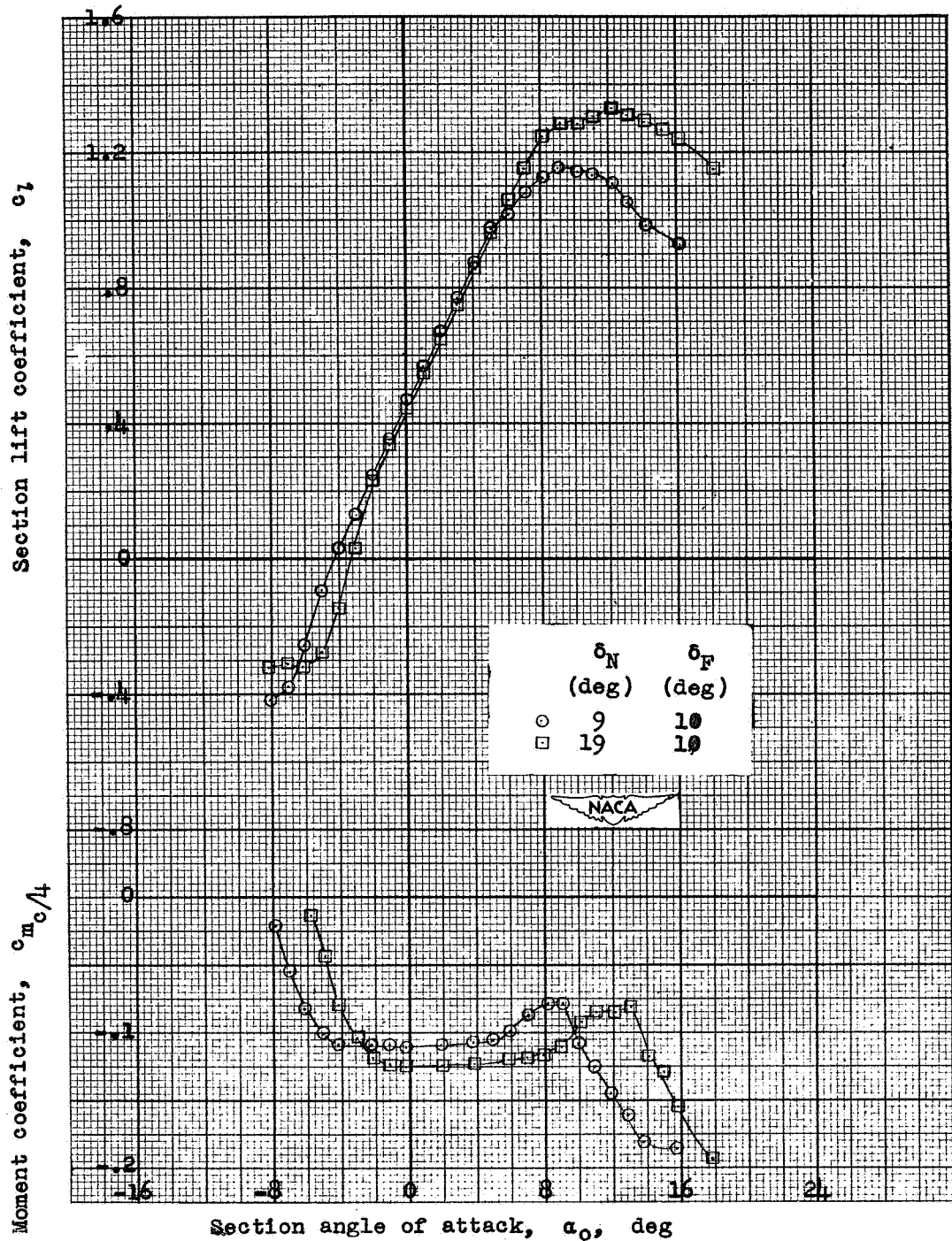


Figure 11.- Section lift and pitching-moment characteristics of an NACA 65A006 airfoil for various deflections of the drooped-nose and plain flaps;  $R, 6 \times 10^6$ .

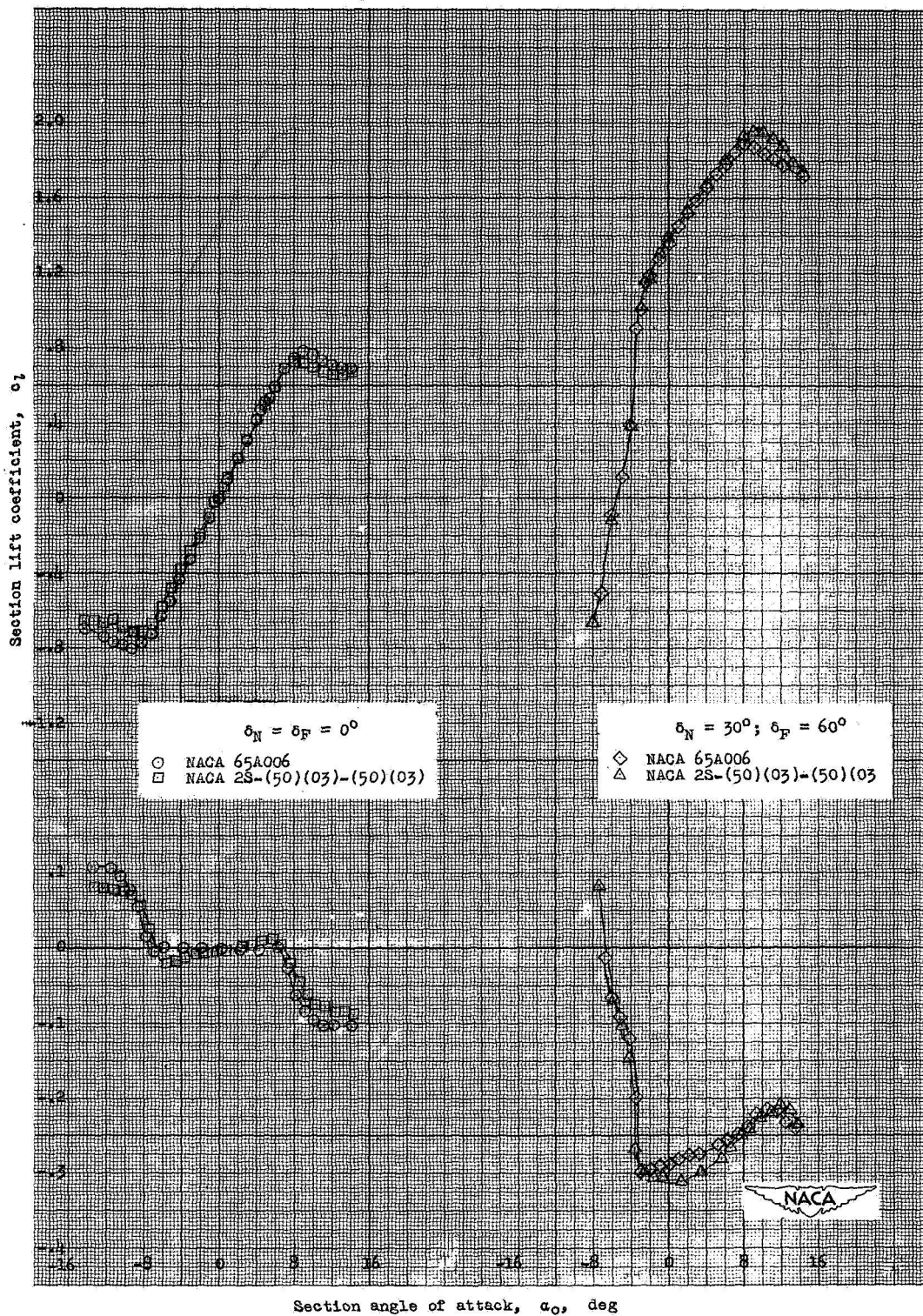


Figure 12.- Comparative lift and pitching-moment characteristics of an NACA 65A006 and an NACA 2S-(50)(03)-(50)(03) airfoil equipped with similar high-lift devices.  $R, 6 \times 10^6$ .